

Georg-August-Universität Göttingen

Iterative and range test method for an inverse source problem for acoustic waves

C. Alves, R. Kress and P. Serranho

Nr. 2008-19

Preprint-Serie des
Instituts für Numerische und Angewandte Mathematik
Lotzestr. 16-18
D - 37083 Göttingen

Iterative and range test method for an inverse source problem for acoustic waves

Carlos Alves*, Rainer Kress† and Pedro Serranho‡

Abstract

We propose two methods for solving an inverse source problem for time-harmonic acoustic waves. Based on the reciprocity gap principle a nonlinear equation is presented for the locations and intensities of the point sources that can be solved via Newton iterations. To provide an initial guess for this iteration we suggest a range test algorithm for approximating the source locations. We give a mathematical foundation for the range test and exhibit its feasibility in connection with the iteration method by some numerical examples.

1 Introduction

The scattering of time harmonic acoustic point sources at n source points with locations s_j and intensities c_j for $j = 1, \dots, n$ at a sound-soft obstacle $D \subset \mathbb{R}^2$ can be modelled by the solution of

$$-\Delta u - k^2 u = \sum_{j=1}^n c_j \delta_{s_j} \quad \text{in } \mathbb{R}^2 \setminus \bar{D}$$

subject to the Dirichlet boundary condition

$$u = 0 \quad \text{on } \partial D$$

*CEMAT and Departamento de Matemática, Instituto Superior Técnico, Lisbon, Portugal

†Institut für Numerische und Angewandte Mathematik, Universität Göttingen, 37083 Göttingen, Germany

‡CEMAT, Instituto Superior Técnico, Lisbon, Portugal and Polytechnical Institute of Leiria, 2411-901 Leiria, Portugal

and the Sommerfeld radiation condition at infinity. Here, δ_s stands for the Dirac delta distribution. This paper is concerned with the inverse problem to recover the location and the intensity of the sources from a knowledge of the normal derivative of u on the boundary ∂D where we assume the boundary ∂D to be known.

We propose an iterative method based on the reciprocity gap principle, that is, on Green's integral theorem. Our approach is motivated by a series of papers using similar ideas for the iterative solution of inverse problems for the shape of the boundary that was initiated by Kress and Rundell [7] for an inverse boundary value problem for the Laplace equation. For a survey of the extension of this approach to the Helmholtz equation we refer to Ivanyshyn, Kress and Serranho [4]. For the case of the inverse source problem the reciprocity gap principle leads to a nonlinear equation for the location and the intensities that can be solved iteratively via simultaneous linearization with respect to all unknowns. Our approach modifies the method considered in [12] through the use of point sources on the boundary ∂D rather than point sources in the exterior $\mathbb{R}^2 \setminus \bar{D}$ of the scatterer. This results in more accurate reconstructions as indicated through our numerical examples. The description of the iterative scheme is provided in Section 3

In order to provide an initial guess for the iterative scheme we propose a range test algorithm for finding approximations for the source locations. For a closed curve Γ containing the closure \bar{D} of the scatterer in its interior we construct a compact linear operator $A : L^2(\Gamma) \rightarrow L^2(\partial D)$ such that the range of A can be used as an indicator whether the source locations are contained in the annulus between Γ and ∂D or not. By choosing different shapes for the curve Γ and numerically deciding via Tikhonov regularization on the solvability of the ill-posed operator equation $A\varphi = f$ for appropriate right hand sides f , depending on the given normal derivative of u , it is possible to approximate the source locations. We will give a detailed analysis of this algorithm in Section 4 including the construction of the operator A and establishing injectivity and dense range as prerequisites for using Tikhonov regularization in the range test. In the final Section 5, numerical examples illustrate the feasibility of the range test and its combination with the iterative scheme. In principle, the approach can of course be extended to three dimensions.

Range test and probe methods have been more recently suggested and developed in inverse scattering for gaining information on the location and shape of scatterers by Luke and Potthast [9] and by Potthast, Sylvester and Kusiak [11]. For a survey we refer to Potthast [10]. However, to our knowledge, this type of methods has not yet been employed for inverse source problems.

In practical remote sensing, faraway sources radiate fields that, within measurement precision, are nearly those radiated by point sources. Hence, the inverse source

problem occurs for example in astronomy. If instead of the exterior problem we consider the interior problem with unknown source locations and intensities within D , then the inverse source problem has applications, for example, in electro- and magneto encephalography. Algorithms like the MUSIC, in principle, also address an inverse source problem but with a different set of data (see for example Kirsch [5]). For related work on the type of inverse problem that we are addressing we refer to Ben Abda et al [1], El Badia and Ha-Duong [3] and Leblond et al [8]

2 The inverse source problem

We proceed with a more specified description of the inverse source problem under consideration. Let $D \subset \mathbb{R}^2$ be a simply connected bounded domain with a C^2 boundary ∂D and outward unit normal ν . Denote by

$$\Phi(x, y) := \frac{i}{4} H_0^{(1)}(k|x - y|), \quad x \neq y,$$

the fundamental solution to the Helmholtz equation with positive wave number k given in terms of the Hankel function of the first kind and of order zero. Consider the direct scattering problem for the sound-soft obstacle D with the incident field u^i generated by a source distribution

$$u^i(x) = \sum_{j=1}^n c_j \Phi(x, s_j), \quad x \neq s_j, \quad j = 1, \dots, n, \quad (2.1)$$

with source points s_j in $\mathbb{R}^2 \setminus \bar{D}$ and intensities $c_j \in \mathbb{C} \setminus \{0\}$ for $j = 1, \dots, n$. The scattered field u^s has to satisfy the Helmholtz equation

$$\Delta u^s + k^2 u^s = 0 \quad \text{in } \mathbb{R}^2 \setminus \bar{D}, \quad (2.2)$$

the sound-soft boundary condition

$$u^i + u^s = 0 \quad \text{on } \partial D \quad (2.3)$$

and the Sommerfeld radiation condition

$$\lim_{r \rightarrow \infty} r^{1/2} \left(\frac{\partial u^s}{\partial r} - i k u^s \right) = 0 \quad (2.4)$$

uniformly for all directions. In the distributional sense, the total field $u := u^i + u^s$ satisfies the inhomogeneous Helmholtz equation

$$-\Delta u - k^2 u = f \quad \text{in } \mathbb{R}^2 \setminus \bar{D}, \quad (2.5)$$

with the inhomogeneity

$$f := \sum_{j=1}^n c_j \delta_{s_j} \quad (2.6)$$

given in terms of the Dirac delta distribution δ_s .

The *inverse source problem* we are interested in is to determine the source locations and intensities, including their number n , from the knowledge of the normal derivative

$$g := \frac{\partial u}{\partial \nu} \quad \text{on } \partial D \quad (2.7)$$

of the total field. We note that this inverse problem is clearly non-linear, since the total field u and therefore its normal derivative g depends non-linearly on the source locations s_j . Moreover, the problem is also ill-posed, since due to the well-posedness of the direct scattering problem for the sound-soft scatterer D , given any $\varepsilon > 0$, we can add a source term with intensity one located far away from the boundary ∂D to f in (2.6) such that difference of the normal derivatives corresponding to the original source f and the perturbed source in the L^2 norm is smaller than ε . In this sense, the solution to the inverse problem does not depend continuously on the data.

We cite the uniqueness result for the inverse problem as considered in Section 3.2 of [12] with a sketch of its proof.

Theorem 2.1 (Uniqueness) *Let*

$$f_1 = \sum_{j=1}^{n_1} c_j^{(1)} \delta_{s_j^{(1)}} \quad \text{and} \quad f_2 = \sum_{j=1}^{n_2} c_j^{(2)} \delta_{s_j^{(2)}}$$

be two source distributions such that for the corresponding total fields u_1 and u_2 as given through the solution of (2.1)–(2.6) for f_1 and f_2 , respectively, and assume that

$$\frac{\partial u_1}{\partial \nu} = \frac{\partial u_2}{\partial \nu} \quad \text{on } \Lambda$$

for some open subset $\Lambda \subset \partial D$. Then $n_1 = n_2$ and $c_j^{(1)} = c_j^{(2)}$ and $s_j^{(1)} = s_j^{(2)}$ for $j = 1, 2, \dots, n_1$.

Proof. The difference $v := u_1 - u_2$ satisfies the differential equation

$$\Delta v + k^2 v = - \sum_{j=1}^{n_1} c_j^{(1)} \delta_{s_j^{(1)}} + \sum_{j=1}^{n_2} c_j^{(2)} \delta_{s_j^{(2)}} \quad \text{in } \mathbb{R}^2 \setminus \bar{D}$$

and the boundary conditions

$$v = 0 \quad \text{on } \partial D$$

and

$$\frac{\partial v}{\partial \nu} = 0 \quad \text{on } \Lambda.$$

By Holmgren's theorem, this implies that

$$v = 0 \text{ in } \mathbb{R}^2 \setminus \left(\bar{D} \cup \left\{ s_j^{(1)} : j = 1, 2, \dots, n_1 \right\} \cup \left\{ s_j^{(2)} : j = 1, 2, \dots, n_1 \right\} \right).$$

Therefore we have that

$$- \sum_{j=1}^{n_1} c_j^{(1)} \delta_{s_j^{(1)}} + \sum_{j=1}^{n_2} c_j^{(2)} \delta_{s_j^{(2)}} = 0$$

and since the Dirac deltas are linearly independent the statement of the theorem follows. \square

Before we proceed with describing our solution algorithm, we note that in the case of the Laplace equation there exists an interesting simplification that connects the exterior inverse source problem to an interior inverse source problem. Denote by

$$\Phi_0(x, y) := \ln \frac{1}{|x - y|}, \quad x \neq y,$$

the fundamental solution for the Laplace equation and consider a disc D of radius one centered at the origin. For any source point $s \in \mathbb{R}^2 \setminus \bar{D}$ we then have the Green's function for the Dirichlet problem given by

$$G(x, y) = \Phi_0(x, y) - \Phi_0(|y|x, |y|y^*)$$

with the reflected point $y^* = |y|^{-2}y \in D$. Hence, for a source point $s \in \mathbb{R}^2 \setminus \bar{D}$ and corresponding $s^* = |s|^{-2}s \in D$. we simulatenously have

$$-\Delta G(\cdot, s) = \delta_s \quad \text{in } \mathbb{R}^2 \setminus \bar{D}$$

and

$$-\Delta G(\cdot, s) = -\delta_{s^*} \quad \text{in } D$$

together with the boundary condition

$$G(\cdot, s) = 0 \quad \text{on } \partial D.$$

Therefore the boundary data produced by a set of external source points $s_j \in \mathbb{R}^2 \setminus \bar{D}$ can be emulated using a corresponding set of internal source points $s_j^* \in D$. Hence, it suffices to solve the internal inverse source problem (see [1, 3, 8]) to recover $s_j^* \in D$ and then by a simple transformation obtain the associated outer sources $s_j \in \mathbb{R}^2 \setminus \bar{D}$. This simplification is no longer possible for the Helmholtz equation. Nevertheless it should be noticed that this procedure may be used to produce an initial guess for the source locations when the wave number is small enough (see [12]).

3 Iterative solution

In [12] an iterative solution method is proposed based on the reciprocity gap principle. Applying Green's theorem in view of the boundary conditions (2.2) and (2.7) it follows that the total field u satisfies

$$\sum_{j=1}^n c_j v(s_j) = \int_{\partial D} v g \, ds \quad (3.1)$$

for all solutions $v \in H_{\text{loc}}^1(\mathbb{R}^2 \setminus \bar{D})$ to the Helmholtz equation satisfying the radiation condition. The method presented in [12] applies the reciprocity gap (3.1) for $v = \Phi(x, \cdot)$ with source locations x on some auxiliary closed curve surrounding ∂D to obtain a set of non-linear equations for the source locations s_j and the intensities c_j .

We suggest to slightly modify this approach and use as test functions v in (3.1) the fundamental solution with source points on the known boundary ∂D instead of source points away from the boundary. As to be expected this improves on the accuracy of the source reconstructions. Putting the source points on the boundary leads to the Green's formula

$$\sum_{j=1}^n c_j \Phi(x, s_j) = \int_{\partial D} \Phi(x, y) g(y) \, ds(y), \quad x \in \partial D, \quad (3.2)$$

which can be seen as a particular case of Huygen's principle, that is, of the representation

$$u = u^i - \int_{\partial D} \frac{\partial u}{\partial \nu}(y) \Phi(x, y), \quad x \in \mathbb{R}^2 \setminus \bar{D},$$

of the total field in Theorem 3.12 in [2] by taking the trace on the boundary ∂D . We use (3.2), or more precisely a discretized version of (3.2), to solve the inverse source problem iteratively by linearizing simultaneously with respect to the intensities and the locations.

Given a current approximation c_1, c_2, \dots, c_n for the intensities and s_1, s_2, \dots, s_n for the locations, we determine updates

$$c_1 + \gamma_1, c_2 + \gamma_2, \dots, c_n + \gamma_n \quad \text{and} \quad s_1 + \xi_1, s_2 + \xi_2, \dots, s_n + \xi_n$$

from the linearized equation

$$\sum_{j=1}^n \{(c_j + \gamma_j)\Phi(x, s_j) + \text{grad}_y \Phi(x, s_j) \cdot \xi_j\} = \int_{\partial D} \Phi(x, y)g(y) ds(y), \quad x \in \partial D. \quad (3.3)$$

This equation is linear with respect to the γ_j and ξ_j . It needs to be solved in a least squares sense after collocating it at a sufficient number of collocation points $x_m \in \partial D$, $m = 1, \dots, M$. For the integral on the right hand side, i.e., the single-layer potential with density g the logarithmic quadrature formulas as described in Section 3.5 of [2] can be employed. Alternatively, one could reformulate (3.2) as a least squares problem and use the Levenberg–Marquardt algorithm, requiring basically the same derivatives.

To start the iterations an initial guess is required for the locations. From this, the initial guess for the intensities can be obtained via solving (3.2) in a least squares sense. Note, that (3.2) is linear with respect to the intensities. An algorithm for providing an initial guess for the source locations is the subject of the next section.

Before we proceed we wish to point out that (3.2), in principle, can also be used for the case of incomplete data, i.e., for the case when g is known only on an open subset $\Lambda \subset \partial D$. In this case, we just consider the missing part $g|_{\partial D \setminus \Lambda}$ as an additional unknown and split the integral over ∂D accordingly. Of course, it is to be expected that this will effect the degree of ill-posedness.

4 Initial guess via a range test

Let B be a simply connected domain with C^2 boundary Γ with outward normal ν such that $\bar{D} \subset B$. We will design a compact linear operator $A : L^2(\Gamma) \rightarrow L^2(\partial D)$ such that the range of A depends on whether the source location are contained in the annulus $G := B \setminus \bar{D}$ or not.

To this end, we denote by $N : L^2(\partial D) \rightarrow H^1(\partial D)$ the Neumann-to-Dirichlet operator for the exterior domain $\mathbb{R}^2 \setminus \bar{D}$ subject to the Sommerfeld radiation condition. Further we denote by u_0 the solution to the exterior Neumann problem with boundary condition

$$\frac{\partial u_0}{\partial \nu} = g \quad \text{on } \partial D. \quad (4.1)$$

In particular, we have $u_0|_{\partial D} = Ng$. Further we introduce the compact operators $V, W : L^2(\Gamma) \rightarrow L^2(\partial D)$ by the single-layer potential

$$(V\varphi)(x) := \int_{\Gamma} \Phi(x, y)\varphi(y) ds(y), \quad x \in \partial D,$$

and its normal derivative

$$(W\varphi)(x) := \int_{\Gamma} \frac{\partial \Phi(x, y)}{\partial \nu(x)} \varphi(y) ds(y), \quad x \in \partial D.$$

If there exist densities $\varphi \in L^2(\Gamma)$ and $\psi \in L^2(\partial D)$ such that the total field u can be represented in the form

$$u(x) = u_0(x) + \int_{\Gamma} \Phi(x, y)\varphi(y) ds(y) + \int_{\partial D} \Phi(x, y)\psi(y) ds(y), \quad x \in G, \quad (4.2)$$

then u is regular in G and therefore none of the source points s_j , $j = 1, \dots, n$, lies within G . Conversely, if none of the source points is contained in G , then $u - u_0$ is regular in G and can be represented as a single-layer potential with density in $L^2(\partial G)$ provided k^2 is not a Dirichlet eigenvalue of the negative Laplacian neither for G nor for D . The latter assumption ensures bijectivity of the single-layer potential operator from $L^2(\partial G)$ to $H^1(\partial G)$.

We abbreviate

$$v(x) := \int_{\Gamma} \Phi(x, y)\varphi(y) ds(y), \quad x \notin \Gamma, \quad (4.3)$$

and

$$w(x) := \int_{\partial D} \Phi(x, y)\psi(y) ds(y), \quad x \notin \partial D.$$

Then, in view of $u = 0$ and $\partial_\nu u = \partial_\nu u_0$ on ∂D by Holmgren's theorem the representation (4.2), that is, the composition $u = u_0 + v + w$ in G , is equivalent to

$$u_0 + v + w = 0 \quad \text{on } \partial D \quad (4.4)$$

and

$$\frac{\partial v}{\partial \nu} + \frac{\partial w}{\partial \nu} = 0 \quad \text{on } \partial D. \quad (4.5)$$

With the aid of the Neumann-to-Dirichlet operator N , that is,

$$w|_{\partial D} + N \left. \frac{\partial v}{\partial \nu} \right|_{\partial D} = 0,$$

we can eliminate w from these two equations and arrive at the ill-posed equation

$$A\varphi = Ng \quad (4.6)$$

for the density φ and the operator $A : L^2(\Gamma) \rightarrow L^2(\partial D)$ given by

$$A := -V + NW. \quad (4.7)$$

Conversely, for a solution $\varphi \in L^2(\Gamma)$ we define v by (4.3). Then we can represent the solution w of the exterior Neumann problem with boundary condition (4.5) as a single-layer potential with density $\psi \in L^2(\partial)$ since the single-layer operator from $L^2(\partial D)$ to $H^1(\partial D)$ is bijective as consequence of our assumption that k^2 is not a Dirichlet eigenvalue for D .

Summarizing we have proven the following theorem.

Theorem 4.1 *Assume that k^2 is not a Dirichlet eigenvalue of the negative Laplacian neither for G nor for D . Then the ill-posed linear integral equation (4.6) is solvable if and only if $s_j \notin G$ for $j = 1, \dots, n$.*

We note that instead of (4.6) we could also use the equivalent equation

$$N^{-1}A\varphi = g \quad (4.8)$$

with the operator

$$N^{-1}A = -N^{-1}V + W$$

where the inverse N^{-1} is given by the Dirichlet-to-Neumann operator.

The idea now is to check the solvability of (4.6), for example, via Tikhonov regularization. If A is injective and has dense range, the regularized solution of (4.6) converges as the regularization parameter tends to zero if and only if (4.6) is solvable (see Section 4 in [2]). Numerically we can test for solvability by performing the Tikhonov regularization for a couple of reasonably small regularization parameters. If the regularized solution remains bounded while the regularization parameter is

decreased then the equation is considered as solvable. Otherwise it is considered as unsolvable.

Here, the assumptions on injectivity and dense range are essential to ensure that the Tikhonov regularization scheme converges to the correct solution rather than to the solution given by the Moore-Penrose inverse. In this sense, we provide the following two theorems.

Theorem 4.2 *The operator A as defined in (4.7) is injective provided k^2 is not a Dirichlet eigenvalue of the negative Laplacian for B .*

Proof. Let $A\varphi = 0$. We define v as single-layer potential by (4.3) and w as the radiating solution to the Helmholtz equation in $\mathbb{R}^2 \setminus \bar{D}$ satisfying the Neumann boundary condition

$$\frac{\partial w}{\partial \nu} = W\varphi \quad \text{on } \partial D,$$

that is,

$$\frac{\partial w}{\partial \nu} = \frac{\partial v}{\partial \nu} \quad \text{on } \partial D.$$

From this we have that

$$w = NW\varphi \quad \text{on } \partial D,$$

whence

$$w = v \quad \text{on } \partial D$$

as consequence of $A\varphi = 0$. Since the Cauchy data of v and w coincide on ∂D and both are analytic in G by Holmgren's theorem we have that

$$v = w \quad \text{in } G.$$

Because the single-layer potential v with density on Γ is analytic in $G \cup \bar{D}$, the function w can be extended across ∂D as a solution to the Helmholtz equation in $G \cup \bar{D}$. Therefore w turns out as entire solution to the Helmholtz equation satisfying the radiation condition. Hence $w = 0$ in all of \mathbb{R}^2 and consequently $v = 0$ in G . This now implies $\varphi = 0$ since by the assumptions on k^2 the single-layer operator from $L^2(\Gamma)$ to $H^1(\Gamma)$ is injective. \square

Theorem 4.3 *The operator A as defined in (4.7) has dense range provided k^2 is not a Dirichlet eigenvalue of the negative Laplacian for D .*

Proof. It suffices to show that the adjoint operator $A^* : L^2(\partial D) \rightarrow L^2(\Gamma)$ of A is injective. Clearly, we have

$$A^* = V^* - W^*N^* \quad (4.9)$$

with the adjoints $V^*, W^* : L^2(\partial D) \rightarrow L^2(\Gamma)$ of V and W , and the adjoint $N^* : L^2(\partial D) \rightarrow L^2(\partial D)$ of $N : L^2(\partial D) \rightarrow L^2(\partial D)$. The adjoints of the potential operators are given by

$$(V^*\psi)(x) := \int_{\partial D} \overline{\Phi(x, y)} \psi(y) ds(y), \quad x \in \partial\Gamma,$$

and

$$(W^*\psi)(x) := \int_{\partial D} \frac{\partial \overline{\Phi(x, y)}}{\partial \nu(y)} \psi(y) ds(y), \quad x \in \partial\Gamma.$$

To characterize the adjoint N^* of the Neumann-to-Dirichlet operator N , given any $\psi_1, \psi_2 \in L^2(\partial D)$, we define w_1 and w_2 as the radiating solutions to the Helmholtz equation in $\mathbb{R}^2 \setminus \bar{D}$ satisfying the Neumann boundary conditions $\partial_\nu w_1 = \psi_1$ and $\partial_\nu w_2 = \overline{\psi_2}$ on ∂D , respectively. By Green's theorem we conclude

$$\int_{\partial D} N\psi_1 \overline{\psi_2} ds = \int_{\partial D} w_1 \frac{\partial w_2}{\partial \nu} ds = \int_{\partial D} w_2 \frac{\partial w_1}{\partial \nu} ds = \int_{\partial D} \psi_1 N \overline{\psi_2} ds,$$

that is,

$$(N\psi_1, \psi_2)_{L^2(\partial D)} = \left(\psi_1, \overline{N\psi_2} \right)_{L^2(\partial D)}.$$

Consequently, N^* is given by

$$N^*\psi = \overline{N\psi}. \quad (4.10)$$

For an explicit form of N , we introduce the operators $S : L^2(\partial D) \rightarrow H^1(\partial D)$ and $K' : L^2(\partial D) \rightarrow L^2(\partial D)$ by

$$(S\psi)(x) := 2 \int_{\partial D} \Phi(x, y) \psi(y) ds(y), \quad x \in \partial D,$$

and

$$(K'\psi)(x) := 2 \int_{\partial D} \frac{\partial \Phi(x, y)}{\partial \nu(x)} \psi(y) ds(y), \quad x \in \partial D.$$

Observing that k is not an interior eigenvalue for D , a single-layer representation of the solution to the exterior Neumann problem leads to the decomposition

$$N = S(-I + K')^{-1} \quad (4.11)$$

for the Neumann-to-Dirichlet operator (cf. [2]). Here, I stands for the identity operator.

We further introduce the operator $T : H^1(\partial D) \rightarrow L^2(\partial D)$ as the normal derivative of the double-layer potential by

$$(T\psi)(x) = 2 \frac{\partial}{\partial \nu(x)} \int_{\partial D} \frac{\partial \Phi(x, y)}{\partial \nu(y)} \psi(y) ds(y), \quad x \in \partial D,$$

and note the identity

$$TS = K'^2 - I \tag{4.12}$$

(see Section 3 in [2] or Section 8 in [6]). From (4.11) and (4.12) we conclude that

$$TN = I + K'. \tag{4.13}$$

After these preparations, we are now ready for proving injectivity of A^* . Let ψ be a solution of $A^*\psi = 0$ and define the potentials

$$v(x) := \int_{\partial D} \Phi(x, y) \overline{\psi(y)} ds(y), \quad x \in \mathbb{R}^2 \setminus \bar{D},$$

and

$$w(x) := \int_{\partial D} \frac{\partial \Phi(x, y)}{\partial \nu(y)} (N\bar{\psi})(y) ds(y), \quad x \in \mathbb{R}^2 \setminus \bar{D}.$$

Then

$$\bar{v}|_{\partial D} = V^*\psi$$

and

$$\bar{w}|_{\partial D} = W^* \overline{N\bar{\psi}} = W^* N^* \psi$$

where we made use of (4.10). From this we observe that $A^*\psi = 0$ implies $v = w$ on Γ . By the uniqueness for the exterior Dirichlet problem and the analyticity of v and w in $\mathbb{R}^2 \setminus \bar{D}$ this implies that $v = w$ in $\mathbb{R}^2 \setminus \bar{D}$, whence

$$\frac{\partial v}{\partial \nu} = \frac{\partial w}{\partial \nu} \quad \text{on } \partial D \tag{4.14}$$

in the sense of the jump relations in the L^2 sense (see Section 3 in [2]). The latter also imply that

$$\frac{\partial v}{\partial \nu} = (-I + K')\bar{\psi}$$

and

$$\frac{\partial v}{\partial \nu} = TN\bar{\psi} = (I + K')\bar{\psi}$$

where we made use of (4.13). In view of the last two equations, from (4.14) we now can conclude that $\psi = 0$ and the proof is complete. \square

Now Theorem 4.1 suggests the following procedure to find the position of the unknown sources. For simplicity assume that ∂D is close to a circle. Then we choose for Γ concentric circles and increase the radius until the equation (4.6) becomes unsolvable in the sense that the L^2 norm of two different Tikhonov solutions to (4.6) for a couple of regularization parameters changes drastically. Then we modify the curve Γ by first decreasing the radius to some extent and then deforming the circle locally by a bump and rotate this bump as we will show in the next section. If for some of these bumpy contours Γ the equation (4.6) is unsolvable we choose a circle containing the corresponding bump. We then solve the equation for the outer domain of these circles. If the equation is solvable, the method for finding an initial guess stops and we choose the center of the circles as initial guesses. Otherwise, we go back to the concentric circles, but now we exclude from G the previous circles around the sources that we found already. Note that in this sense, in principle, our approach can be interpreted as a range test algorithm for finding the sources.

5 Numerical examples

In our examples we confine ourselves to the case where D is a disk of radius one centered at the origin and to the wave number $k = 1$. For the numerical discretization of the right hand side in (3.2) and of the Neumann-to-Dirichlet operator (4.11) we used the logarithmic quadrature rules in [2] with 80 quadrature points over the boundary ∂D . The synthetic data were generated by using the combined single- and double-layer approach for solving the direct problem. Note that no inverse crime can be committed since the algorithm for the inverse problem does not contain the integral equations used for the solution of the direct problem.

We will present numerical results both for the range test method for finding an initial guess and for the iterative method.

5.1 Range test method for initial guess

First we describe the numerical implementation of the range test method as suggested at the end of the previous Section 4. We start by choosing Γ as a concentric circle with radius 2 and then increase the radius by one until the equation becomes unsolvable. To test solvability, we solve equation (4.6) by Tikhonov regularization with regularization parameters $\alpha_1 = 10^{-8}$ and $\alpha_2 = 10^{-12}$. We consider the equation (4.6) to be unsolvable if the relative L^2 error between the two solutions for the different regularization parameters is larger than 50%. For the discretization of the integrals over Γ we used the trapezoidal rule with 120 quadrature points.

After we obtain a circle for which unsolvability occurs we consider bumpy curves parametrized by

$$p(t) = \left(r + \frac{3}{2} e^{-4n\sqrt{r}\sin^2\frac{t}{2}} \right) \{ \cos(t - \theta), \sin(t - \theta) \}$$

where r is the largest radius of the concentric circle for which the equation (4.6) was solvable, $2n$ is the number of bumpy curves used for fixed radius r and θ is an angle describing the location of the bump. The number

$$n = \text{round} \left(\frac{5r}{4} \right)$$

seems to be a good empirical choice along with $2n$ equidistant angles $\theta_j = \frac{\pi j}{n}$, $j = 1, 2, \dots, 2n$, in order to cover most of the annulus between the circles of radii r and $r+1$. For each θ_i for which the equation (4.6) was not solvable we picked the circle with radius $\frac{5}{4}$ centered at $-\left(r + \frac{3}{10}\right) \{ \cos \theta_i, \sin \theta_i \}$ to exclude the corresponding source.

5.1.1 First example: One source

As a first example we considered a single source located at $s_1 = (4, 0)$ with intensity 1, that is, the incident field is given by $u^i(x) = \Phi(x, (4, 0))$. We applied the range test algorithm with the configuration as described above and the result is plotted in Figure 2. The disk that was obtained indeed covers the unknown source and the center of the circle can be used as an initial guess for the iterative method.

5.1.2 Second example: Three sources

To the source $s_1 = (4, 0)$ with intensity $c_1 = 1$ from the previous example we added two more sources at $s_2 = (-3, 1)$ and $s_3 = (-2, 4)$ with intensities $c_2 = 3$

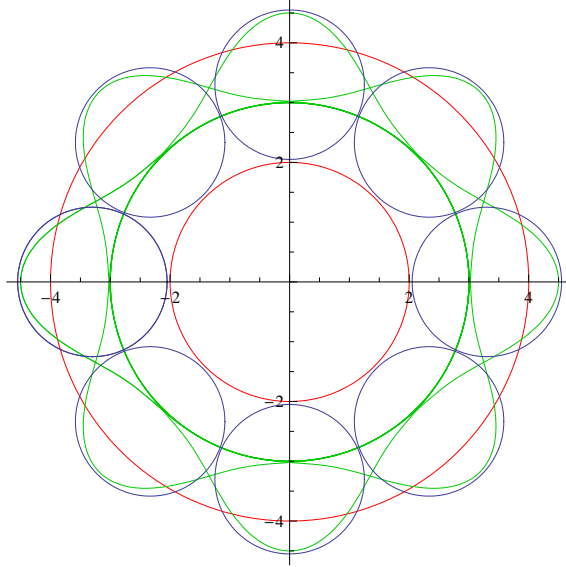


Figure 1: For $r = 3$ concentric circles of radius $r - 1$ and $r + 1$ are shown in red, circles with bumps in green and circles centered at the bumps in blue for all $\theta_i, i = 1, 2, \dots, 2n$.

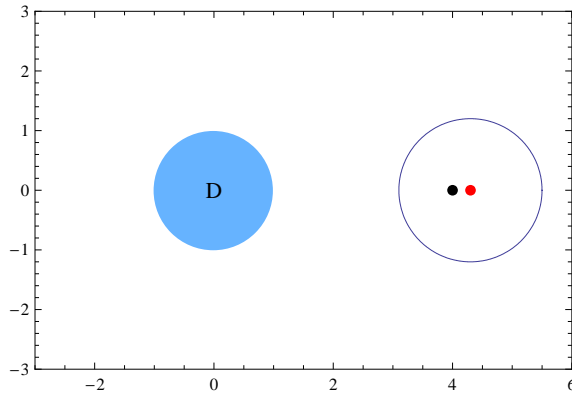


Figure 2: Circle centered in the red dot covers the unknown source (black dot) for the data of the first example.

and $c_3 = -2$, respectively, that is, we considered the incident field

$$u^i(x) = \Phi(x, (4, 0)) - 2\Phi(x, (-2, 4)) + 3\Phi(x, (-3, 1)).$$

Applying the range test algorithm, again the disks cover the unknown sources as presented in Figure 3.

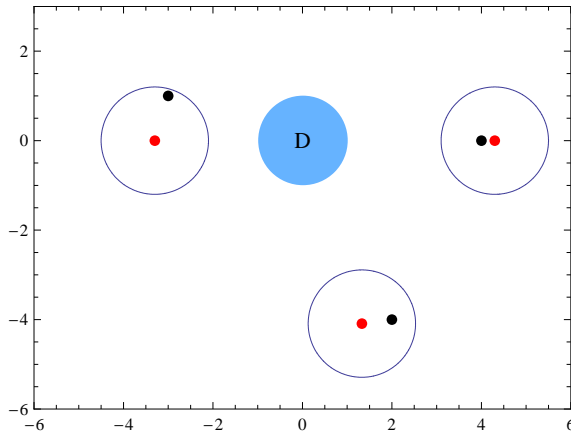


Figure 3: Circles centered in the red dots cover the unknown sources (black dots) for the data of the second example.

However we should note some restrictions of our approach. The circles considered to exclude the sources do not cover all the plane and therefore the method (as applied here) might not work in some cases. A more complete coverage of the plane by disjoint sets with well behaved boundaries would then be needed and we leave this for future research. We also might have the situation where two or more sources lie within a circle, that is, our method does not actually separate all the sources. However, this could be taken into account by taking several initial guesses inside each circle for the iterative method. We also point out that our method has some difficulties in finding sources away from the obstacle, which is due to the ill-posed nature of the problem as pointed out above. Finally, we admit that as it is obvious from its construction the range test algorithm is very sensitive to noisy data.

5.2 Iterative method

We now illustrate the application of the iterative method as presented in Section 3 using as initial guess the approximations for the source locations from the previous subsection. As a stopping criteria for the iterations we used an adaptation of Morozov's discrepancy principle, that is, we stopped the at the m -th iteration if the

residual

$$e^{(m)} = \left\| \frac{\partial u^{(m)}}{\partial \nu} - g \right\|_{L^2(\partial D)}$$

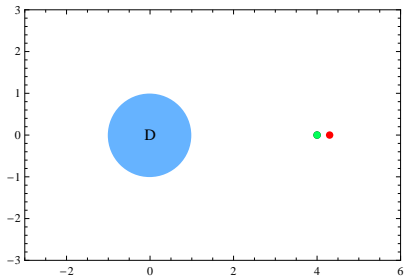
is larger than for the previous iteration. Here $\partial_\nu u^{(m)}$ denotes the normal derivative on ∂D of the total field generated by the current approximation for the incident field with approximations $s_j^{(m)}$ for the source locations and approximations $c_j^{(m)}$ for the source intensities. To solve equation (3.3) we applied Tikhonov regularization with regularization parameter

$$\alpha = 0.1\alpha_0^m, \quad \alpha_0 = \min\{0.9, 0.55 + 15n_l\}$$

for the m -th iteration with the noise level n_l . In this way the regularization parameter decreases with the number of iterations at a slower rate for higher noise level.

5.2.1 First example: One source

Again we considered a single source located at $(4, 0)$ with intensity 1. We first worked with exact data using as initial guess the center of the circle obtained in Section 5.1.1. The result as presented in Figure 4 is extremely accurate with an error of order 10^{-8} for the source location.

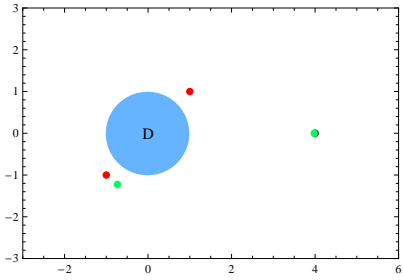


s_1	\tilde{s}_1
$\{4, 0\}$	$\{4 - 2 \times 10^{-9}, 5 \times 10^{-17}\}$
c_1	\tilde{c}_1
1	$1 + 10^{-6} + 7 \times 10^{-9}i$

Number of iterations: 14

Figure 4: Left: Initial guess red, exact location black and approximation (no noise) green (superposing the black dot). Right: Table with corresponding values.

We also applied the method with 1% and 5% noise on the data, using as initial guess two sources located at $\tilde{s}_1 = (1, 1)$ and $\tilde{s}_2 = (-1, -1)$, both with intensity 1, that is, with an incorrect number of sources in the initial guess. The results in Figures 5 and 6 show that the source \tilde{s}_1 approximates the existing source, while the intensity of the second source tends to zero. The errors are of the same order as the noise level as to be expected from Morozov's principle.

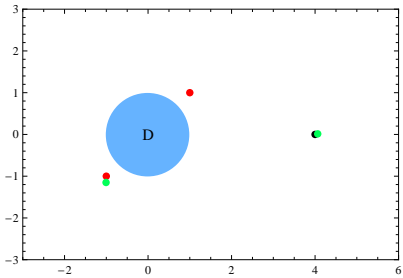


j	s_j	\tilde{s}_j
1	{4, 0}	(3.980, 0.001)
2	-	(-0.733, -1.225)

j	c_j	\tilde{c}_j
1	1	0.997 + 0.019i
2	-	-0.00020 - 0.00006i

Number of iterations: 24

Figure 5: Left: Initial guess red, exact location black and approximation (1% noise) green. Right: Table with corresponding values.



j	s_j	\tilde{s}_j
1	(4, 0)	(4.064, 0.0134)
2	-	(-1.005, -1.149)

j	c_j	\tilde{c}_j
1	1	1.006 - 0.066i
2	-	0.00048 - 0.00068i

Number of iterations: 22

Figure 6: Left: Initial guess red, exact location black and approximation (5% noise) green. Right: Table with corresponding values.

5.2.2 Second example: Three sources

We go back to the example in Subsection 5.1.2, that is, we want to recover the locations and intensities of the sources generating the incident field

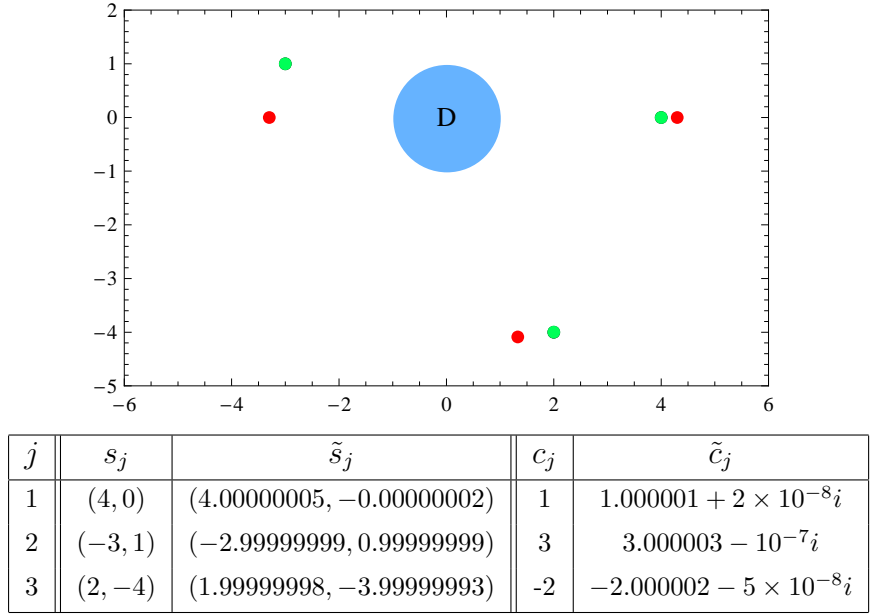
$$u^i(x) = \Phi(x, (4, 0)) + 3\Phi(x, (-3, 1)) - 2\Phi(x, (-2, 4)).$$

Again we start by applying the method with exact data using as initial guess the centers of the circles obtained in Subsection 5.1.2. The result is presented in Figure 7, an extremely accurate reconstruction is exhibited again.

Analogously to the previous example we applied the method with 1% and 5% noise on the data, using as initial guess four sources located at

$$\tilde{s}_1 = (1, 1), \quad \tilde{s}_2 = (-1, 1), \quad \tilde{s}_3 = (1, -1), \quad \tilde{s}_4 = (-1, -1),$$

all with intensity 1. In a similar way, the results in Figures 8 and 9 show that three



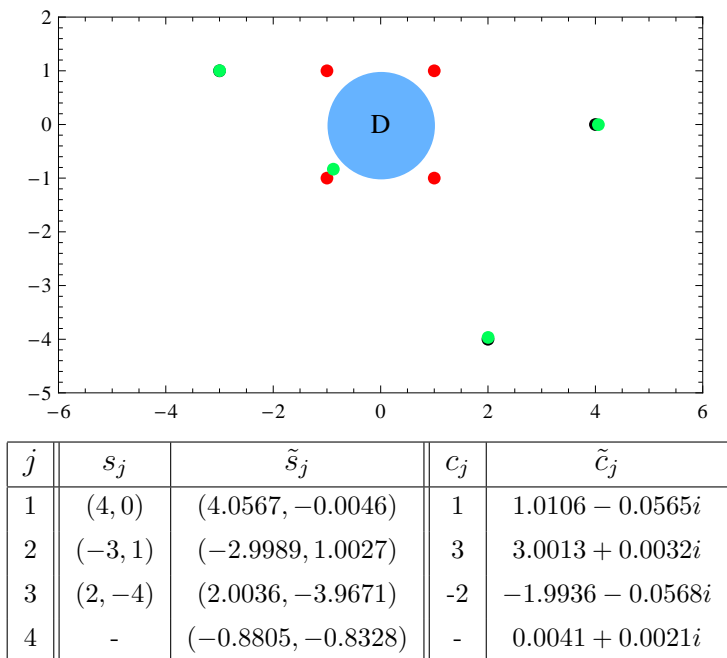
Number of iterations: 20

Figure 7: Top: Initial guess in red, exact location in black and approximation in green (no noise) for Example 5.2.2 on top. Bottom: Table of approximations.

of the sources approximate the existing sources, while the intensity of the remaining source is close to zero.

6 Conclusion

We have proposed and analysed a combination of a range test algorithm and an iterative scheme based on the reciprocity gap principle for the inverse source problem. Numerical examples provide evidence for the feasibility of this approach. Further research is required to make the method more efficient and to extend it to three dimensions. In principle, the method can also be applied to other boundary conditions than the sound-soft scatterer, to interior problems and to other differential equations.



Number of iterations: 41

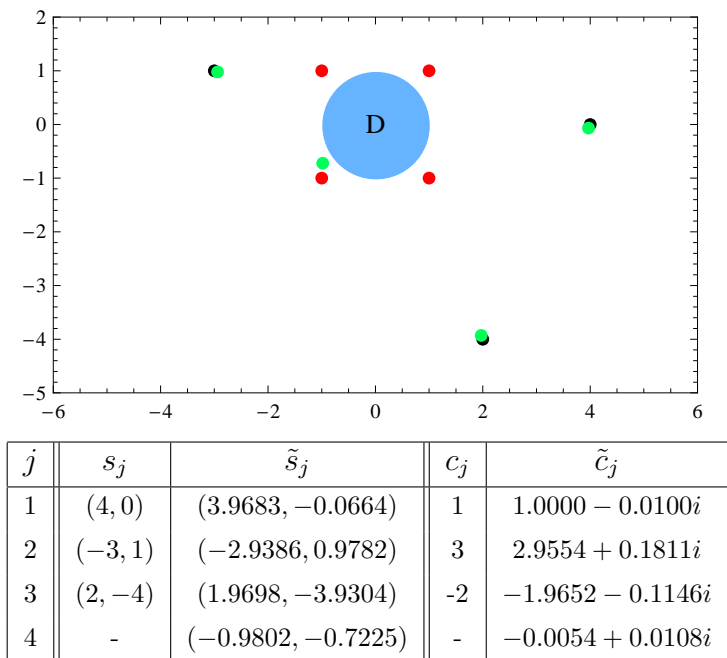
Figure 8: Top: Initial guess in red, exact location in black and approximation in green (1% noise) for Example 5.2.2. Bottom: Table of approximations.

Acknowledgments

C. Alves acknowledges the support by the FCT project POCI/MAT/60863/2004. P. Serranho acknowledges the support of his research by *Fundação Calouste Gulbenkian*. This work was initiated during visits of R.K. at the Instituto Superior Técnico in Lisbon and of P.S. at the University of Göttingen. The support and the hospitality are gratefully acknowledged.

References

- [1] Ben Abda, A., Ben Hassen, F., Leblond, J. and Majoub, M.: Sources recovery from boundary data: a model related to electroencephalography. *Mathematical and Computer Modelling*, to appear.
- [2] Colton, D. and Kress, R.: *Inverse Acoustic and Electromagnetic Scattering Theory*. 2nd. ed. Springer-Verlag, Berlin Heidelberg New York, 1998.



Number of iterations: 76

Figure 9: Top: Initial guess in red, exact location in black and approximation in green (5% noise) for Example 5.2.2. Bottom: Table of approximations.

- [3] El Badia, A and Ha-Duong, T.: An inverse source problem in potential analysis Inverse Problems **16**, 651–663 (2000).
- [4] Ivanyshyn, O., Kress, R. and Serranho, P.: Huygen’s principle and iterative methods in inverse obstacle scattering. (to appear)
- [5] Kirsch, A.: The MUSIC algorithm and the factorization method in inverse scattering theory for inhomogeneous media. Inverse Problems **18**, 1025–40 (2002).
- [6] Kress, R.: *Linear Integral Equations*, 2nd. ed. Springer-Verlag, Berlin Heidelberg New York, 1999.
- [7] Kress, R. and Rundell, W.: Nonlinear integral equations and the iterative solution for an inverse boundary value problem. Inverse Problems **21**, 1207–1223 (2005).
- [8] Leblond, J., Paduret, C., Rigat, S. and Zghal, M. Source localization in ellipsoids by the best meromorphic approximation in planar sections Inverse Problems **24**, 035017 (2008).

- [9] Luke, R. and Potthast, R.: The No Response Test-A Sampling Method for Inverse Scattering Problems Siam J. Appl.Math (2003).
- [10] Potthast, R.: A survey on sampling and probe methods for inverse problems. Inverse Problems **22**, R1–R47 (2006).
- [11] Potthast, P., Sylvester, J. and Kusiak, S.: A range test for determining scatterers with unknown physical properties Inverse Problems **19**, 533–547 (2003).
- [12] Vasconcelos, A.: *Detection of Outer Sound Sources Through Measurements of Amplitude on a Body Surface*. MSc Thesis. Instituto Superior Técnico, Lisbon, 2007.

Institut für Numerische und Angewandte Mathematik
Universität Göttingen
Lotzestr. 16-18
D - 37083 Göttingen

Telefon: 0551/394512
Telefax: 0551/393944

Email: trapp@math.uni-goettingen.de URL: <http://www.num.math.uni-goettingen.de>

Verzeichnis der erschienenen Preprints 2008:

2008-01	M. Körner, A. Schöbel	Weber problems with high-speed curves
2008-02	S. Müller, R. Schaback	A Newton Basis for Kernel Spaces
2008-03	H. Eckel, R. Kress	Nonlinear integral equations for the complete electrode model in inverse impedance tomography
2008-04	M. Michaelis, A. Schöbel	Integrating Line Planning, Timetabling, and Vehicle Scheduling: A customer-oriented approach
2008-05	O. Ivanyshyn, R. Kress, P. Serranho	Huygen's principle and iterative methods in inverse obstacle scattering
2008-06	F. Bauer, T. Hohage, A. Munk	Iteratively regularized Gauss-Newton method for nonlinear inverse problems with random noise
2008-07	R. Kress, N. Vintonyak	Iterative methods for planar crack reconstruction in semi-infinite domains
2008-08	M. Uecker, T. Hohage, K.T. Block, J. Frahm	Image reconstruction by regularized nonlinear inversion - Joint estimation of coil sensitivities and image content
2008-09	M. Schachtebeck, A. Schöbel	IP-based Techniques for Delay Management with Priority Decisions
2008-10	S. Cicerone, G. Di Stefano, M. Schachtebeck, A. Schöbel	Dynamic Algorithms for Recoverable Robustness Problems
2008-11	M. Braack, G. Lube	Finite elements with local projection stabilization for incompressible flow problems
2008-12	T. Knopp, X.Q. Zhang, R. Kessler, G. Lube	Enhancement of an Industrial Finite-Volume Code for Large-Eddy-Type Simulation of Incompressible High-Reynolds Number Flow Using near-Wall Modelling
2008-13	P. Knobloch, G. Lube	Local projection stabilization for advection-diffusion-reaction problems: One-level vs. two-level approach

2008-14	G. Lube, B. Tews	Distributed and boundary control of singularly perturbed advection-diffusion-reaction problems
2008-15	G. Lube, B. Tews	Optimal control of singularly perturbed advection-diffusion-reaction problems
2008-16	M. Weyrauch, D. Scholz	Computing the Baker-Campbell-Hausdorff series and the Zassenhaus product
2008-17	A. Schöbel, D. Scholz	The big cube small cube solution method for multidimensional facility location problems
2008-18	X. Zhang, T. Knopp, M. Valentino, R. Kessler, G. Lube	Investigation of resolution requirements for wall-modelled LES of attached and massively separated flows at high Reynolds numbers
2008-19	C. Alves, R. Kress, P. Serranho	Iterative and range test method for an inverse source problem for acoustic waves

latex hinten-2008.tex